

Angular Signatures for Galactic Halo WIMP Scattering in Direct Detectors: Prospects and Challenges

Craig J. Copi¹ and Lawrence M. Krauss^{1,2}

¹*Department of Physics,* ²*Department of Astronomy*

Case Western Reserve University, 10900 Euclid Ave., Cleveland OH 44106-7079

(November 4, 2018)

CWRU-P8-00

Angular Sensitivity can provide a key additional tool which might allow unambiguous separation of a signal due to Galactic halo WIMPs from other possible backgrounds in direct detectors. We provide a formalism which allows a calculation of the expected angular distribution of events in terrestrial detectors with angular sensitivity for any incident distribution of Galactic halo dark matter. This can be used as an input when studying the sensitivity of specific detectors to halo WIMPs. We utilize this formalism to examine the expected signature for WIMP dark matter using a variety of existing analytic halo models in order to explore how uncertainty in the Galactic halo distribution impact on the the event rates that may be required to separate a possible WIMP signal from other terrestrial backgrounds. We find that as few as 30 events might be required to disentangle the signal from backgrounds if the WIMP distribution resembles an isothermal sphere distribution. On the other hand, for certain halo distributions, even detectors with fine scale resolution may require in excess of a 100-400 events to distinguish a WIMP signal from backgrounds using angular sensitivity. We also note that for finite thresholds the different energy dependence of spin-dependent scattering cross sections may require a greater number of events to discern a WIMP signal than for spin independent interactions. Finally, we briefly describe ongoing studies aimed at developing strategies to better exploit angular signatures, and the use of N-body simulations to better model the expected halo distribution in predicting the expected signature for direct WIMP detectors.

I. INTRODUCTION

The effort to directly detect Galactic halo weakly interacting massive particles (WIMPs) which may form the dark matter dominating our Galaxy is now entering a new phase. Numerous experiments are now operating with a sensitivity to scattering cross sections in the range predicted for low energy SUSY neutralinos [1–3], and indeed one such experiment has claimed a preliminary detection [4].

There is a problem however, with existing detection schemes, which the controversy over the recent DAMA results underscores. The signature for elastic scattering of WIMPs on nuclear targets involves the observation of what is essentially excess noise in the detector. Thus, in order to definitively establish a positive detection, one has to convincingly demonstrate that this excess noise is indeed WIMP induced, and not due to some unexpected terrestrial background. The signature focussed on by the DAMA collaboration, an annual modulation due to the Earth's orbital motion through the WIMP halo, is problematic in this regard. In the first place, the effect is small, at the few percent level at best [5]. In addition, numerous radioactive backgrounds are known to modulate over the course of a year.

The Earth's motion around the Sun, combined with the Sun's motion around the Galactic disk, can however provide another, much larger and more unambiguous signature. If detectors can be developed that are sensitive to the direction of recoil of the nucleus impacted by a WIMP, then the expected signal will have an angular dependence characteristic of this velocity relative to the incident WIMP halo phase space distribution.

For a simple isothermal sphere distribution, the resulting angular differential rates can be easily calculated [6], and it is clear that a large forward-backward asymmetry can be produced. However, it is quite likely that the actual Galactic halo WIMP distribution is not well represented by such a simple analytical approximation. Building detectors with angular sensitivity is a daunting challenge, although testing of at least one such proposed detector, the DRIFT detector [7,8] is currently underway. It is therefore appropriate to explore in advance to what extent uncertainties in our knowledge of a halo WIMP distribution will have on the detector parameters required required to separate a WIMP signal from other backgrounds.

Recently we outlined a comprehensive formalism which allows the generation of expected angular event rates in terrestrial detectors with angular sensitivity for any incident WIMP distribution, and made a provisional exploration of the overall event rates required in detectors for simple halo models in order to separate the signal from a flat background

[9]. Here, we follow up by providing a detailed derivation and description of our results, and also by incorporating a much broader spectrum of analytical halo models. In addition, we also make a provisional analysis of the possible effects of spin-dependence of WIMP-nucleon cross sections on the resulting angular signatures. Finally, we briefly describe ongoing work aimed at incorporating more realistic WIMP distributions arising from N-body simulations into our analysis, and applying our results to various specific proposed detectors, where energy-dependence of both signals and backgrounds may play a key role. Our present results, however, point out the challenges of discerning an angular signal in advance of specific knowledge of the halo WIMP distribution. In addition, the formalism provided here can be used to generate angular event rates which can in turn be used by experimental groups as an input into their detector Monte Carlo analyses.

The outline of this work is as follows: First, in section II, we present a detailed derivation of the differential angular cross sections in a terrestrial laboratory frame for any incident WIMP distribution. In section III we discuss a broad range of different analytical halo models that have been proposed in the literature, and outline the relevant parameter ranges of importance for influencing the resulting angular signature for WIMP scattering. In this section we also incorporate effects of the detailed motion of the Earth in a Galactic-rest frame, and also examine the effect of incorporating possible spin-dependence of WIMP-nucleus scattering on the resulting angular signals, as well as briefly outlining the generic detector and WIMP parameters we used in generating our results. In section IV we present the results for the expected angular distributions in these model detectors. In section V we then proceed to describe the Monte Carlo analysis we performed to determine the required event rates in order to separate signals from backgrounds for the different halo and detector models. In section VI we summarize our conclusions, and describe ongoing efforts to further refine our analyses and predictions.

II. DIFFERENTIAL EVENT RATES

The WIMP rate as a function of recoil energy for various WIMP models has been carefully studied over the past decade (see [1] for a review). The angular dependence of the event rate, assuming an incident spherically symmetric isothermal halo WIMP distribution has also been discussed. [6,10]. In order to explore a more general class of halo distributions, in particular those which might not be spherically these formalisms are not adequate, however, and one must generalize them [9]. We present the derivation of such a generalized formalism here.

The event rate of WIMPs depends on their local density, ρ_0 , and their velocity distribution in the halo, $f(\mathbf{v})$. Assume the WIMPs have a uniform spatial density on the scale of the Earth's motion through the halo over the course of one year. The event rate is then simply given by

$$R \sim \frac{n\sigma}{m_n} \langle v \rangle, \quad (1)$$

where m_n is the mass of the nuclear target, m_χ is the mass of the WIMP, $n = \rho_0/m_\chi$ is the number density of WIMPs, σ is the cross section, and $\langle v \rangle$ is the average velocity of the WIMPs relative to the detector.

Consider a WIMP of mass m_χ moving with velocity $\mathbf{v} = v(\hat{x} \sin \alpha \cos \beta + \hat{y} \sin \alpha \sin \beta + \hat{z} \cos \alpha)$ in the laboratory frame (figure 1). Let this WIMP scatter off a nucleus of mass m_n in the direction (θ^*, ξ) in the center-of-mass frame. The recoil energy of the nucleus is

$$Q = \frac{m_n m_\chi^2}{(m_n + m_\chi)^2} v^2 (1 - \mu), \quad (2)$$

where $\mu = \cos \theta^*$. Let $\mathbf{u} = u(\hat{x} \sin \gamma \cos \phi + \hat{y} \sin \gamma \sin \phi + \hat{z} \cos \gamma)$ be the recoil velocity of the nucleus in the laboratory frame (figure 1). To determine the relations among these sets of angles we begin by considering the simplified scattering problem of a WIMP incident along the z -axis. We can then rotate this result for an arbitrary WIMP incident at an angle (α, β) to find (in the non-relativistic limit)

$$\begin{aligned} \cos \gamma &= \sqrt{\frac{1-\mu}{2}} \cos \alpha - \sqrt{\frac{1+\mu}{2}} \sin \alpha \cos \xi, \\ \sin \gamma \cos \phi &= \sqrt{\frac{1-\mu}{2}} \sin \alpha \cos \beta - \sqrt{\frac{1+\mu}{2}} (\sin \beta \sin \xi - \cos \alpha \cos \beta \cos \xi), \\ \sin \gamma \sin \phi &= \sqrt{\frac{1-\mu}{2}} \sin \alpha \sin \beta + \sqrt{\frac{1+\mu}{2}} (\cos \beta \sin \xi + \cos \alpha \sin \beta \cos \xi). \end{aligned} \quad (3)$$

Notice in the limit of $(\alpha, \beta) \rightarrow (0, 0)$ this reduces to the usual two dimensional result.

To remove the dependence on the center of mass angles we note that

$$\sin \frac{\theta^*}{2} = \sqrt{\frac{1-\mu}{2}} = |\cos \gamma \cos \alpha + \sin \gamma \sin \alpha \cos(\beta - \phi)| \quad (4)$$

and the Jacobian

$$\frac{\partial(\cos \gamma, \phi)}{\partial(\mu, \xi)} = \frac{1}{4} \sqrt{\frac{2}{1-\mu}}. \quad (5)$$

Next, to simplify subsequent formulae, we define a geometrical factor, J , by

$$\begin{aligned} J(\alpha, \beta; \gamma, \phi) &\equiv \frac{\mathbf{u} \cdot \mathbf{v}}{|\mathbf{u}||\mathbf{v}|} = \frac{1}{4} \left| \frac{\partial(\cos \gamma, \phi)}{\partial(\mu, \xi)} \right|^{-1} \\ &= \cos \alpha \cos \gamma + \sin \alpha \sin \gamma \cos(\beta - \phi). \end{aligned} \quad (6)$$

With this information we can now write the event rates solely as a function of the incoming lab angle (α, β) and the recoiling lab angle (γ, ϕ) .

The event rate per nucleon in the detector is given by

$$dR = f(v, \alpha, \beta) v^3 dv d(\cos \alpha) d\beta \frac{d\sigma}{d\mu} d\mu \frac{d\xi}{2\pi}. \quad (7)$$

Here we will assume the nucleon-WIMP scattering has the form

$$\frac{d\sigma}{d\mu} = \frac{\sigma_0}{2} F^2(Q), \quad (8)$$

where $F^2(Q)$ is the form factor and σ_0 is energy independent. The number of events in which a nucleus recoils with energy Q is

$$\frac{dR}{dQ} = \frac{\sigma_0 \rho_0}{2m_r^2 m_n} F^2(Q) \int_{v_{\min}}^{v_{\text{esc}}} v dv \int d\Omega_{\alpha, \beta} f(v, \alpha, \beta), \quad (9)$$

where v_{esc} is the escape velocity of the Galaxy, $v_{\min}^2 = \frac{(m_\chi + m_n)^2}{2m_\chi^2 m_n} Q$ is the minimum incident WIMP velocity that can produce a nuclear recoil of energy Q , and $m_r = m_\chi m_n / (m_\chi + m_n)$ is the reduced mass. This formula is well known and, in the case of an isothermal model when we only consider the projected motion of the Earth along the Sun's velocity, it can be evaluated analytically.

In this work we are most interested in the angular dependent event rate which is found to be

$$\frac{dR}{d\Omega_{\gamma, \phi}} = \frac{\sigma_0 \rho_0}{\pi m_n m_\chi} \int_{v_{\min}/J}^{v_{\text{esc}}} v^3 dv F^2(Q(v, J)) \int d\Omega_{\alpha, \beta} f(v, \alpha, \beta) J(\alpha, \beta; \gamma, \phi) \Theta(J). \quad (10)$$

Here $\Theta(J)$ is the usual step function and J is the geometrical factor discussed above (6) that relates the incident WIMP direction to the recoiled nucleus direction.

We can further derive the event rate as a function of both the deposited energy and the recoil angle,

$$\frac{d^2 R}{dQ d\Omega_{\gamma, \phi}} = \frac{m_n \sigma_0 \rho_0}{8\pi m_r^4 m_\chi} Q F^2(Q) \int d\Omega_{\alpha, \beta} f(v(Q, J), \alpha, \beta) \frac{\Theta(J)}{J^3}. \quad (11)$$

In principle this would provide the most information allowing for the best separation of signal from background. Note, however, that in order to fully exploit this signature some detector-specific estimation of the energy dependence of various backgrounds must be given.

In this work we will focus on the angular event rate, which does not require a knowledge of the specific energy dependent detector backgrounds in order to explore the separation of signals from backgrounds. Exploiting the full distribution for various proposed detectors will be analyzed in future work.

III. MODEL PARAMETERS

Armed with the above differential event rates we can now analyze a wide variety of halo models, form factors, WIMP parameters, detector parameters, *etc.* Here we will discuss the parameters considered in this study.

A. Halo Models

A standard spherically symmetric isothermal sphere reproduces the large scale features of the flat rotation curves around galaxies. However, numerous dynamical arguments suggest that actual halo model may not be well described by such a distribution. As a result, a variety of more complex analytical models have been developed. The models we discuss here can be considered to be of three types: smooth axisymmetric, smooth triaxial, and clumped. The first type includes a standard spherical isothermal WIMP halo, as well as a modified axisymmetric halo, both rotating and non-rotating. Most recently a general triaxial generalization of the spherical isothermal halo has been developed. As an example of the last type of halo model, which ultimately should include realistic halo distributions arising from accretion of sub-systems by the growing galaxy, we consider a caustic model recently developed by Sikivie. While all of these models are analytic approximations, they do represent a broad spectrum of different possibilities, which should give some idea of the range of uncertainty in the predicted angular distributions in detectors.

1. Isothermal Model

A simple spherically symmetric isothermal distribution is given by,

$$f(\mathbf{v}) = \frac{1}{\pi^{3/2}v_0^3} e^{-|\mathbf{v}|^2/v_0^2}. \quad (12)$$

Here $\langle v^2 \rangle^{1/2} = \sqrt{3/2}v_0$ is the dispersion velocity of the dark matter in the halo. Note that we can allow different dispersions in each direction but will not pursue that option further. The standard value chosen for v_0 is 220 km/s. We will consider the range of values $v_0 = 150$ km/s, 220 km/s, and 300 km/s here.

2. Axisymmetric Halo Model

The Evans model [11] is an axisymmetric halo model that allows for flattening. This model has been studied in the context of annular modulations by Kamionkowski and Kinkhabwala [12]. The distribution function is given by

$$f(\mathbf{v}) = \frac{1}{D^2} \left[AR_0 (v \cos \alpha - v_{\oplus,x})^2 + B \right] e^{-2(v-\Psi)^2/v_0^2} e^{-2v_{\oplus}^2 - \Psi^2/v_0^2} + \frac{C}{D} e^{-(v-\Psi)^2/v_0^2} e^{-v_{\oplus}^2 - \Psi^2/v_0^2}, \quad (13)$$

where

$$A = \left(\frac{2}{\pi}\right)^{5/2} \frac{1-q^2}{Gq^2v_0^3}, \quad B = \sqrt{\frac{2}{\pi^5}} \frac{R_c^2}{Gq^2v_0}, \quad C = \frac{2q^2-1}{4\pi Gq^2v_0},$$

$$D = R_c^2 + R_0^2, \quad \Psi = v_{\oplus,x} \cos \alpha + v_{\oplus,y} \sin \alpha \cos \beta + v_{\oplus,z} \sin \alpha \sin \beta, \quad (14)$$

R_c is the core radius, R_0 is the distance of our solar system from the center of the Galaxy, v_0 is the circular speed at large radii, and q is the flattening parameter ranging from $q = 1$ to $q = 1/\sqrt{2}$. In this work we adopt $R_c = 7$ kpc, $R_0 = 8.5$ kpc, and $v_0 = 220$ km/s. The most important parameter is the flattening, q . Here we choose $q = 1$ (cored isothermal model), 0.85, and $1/\sqrt{2}$ (maximum flattening).

3. Triaxial Halo Models

Constructing velocity distributions from general triaxial halos is a difficult problem. Evans, Carollo, and de Zeeuw [13] have provided such distributions for the logarithmic ellipsoidal potential; the simplest triaxial model and a natural generalization of the isothermal sphere. In this case we can approximate the velocity distribution as

$$f(\mathbf{v}) = \frac{1}{\pi^{3/2}\sigma_x\sigma_y\sigma_z} \exp \left[-\frac{v_x^2}{\sigma_x^2} - \frac{v_y^2}{\sigma_y^2} - \frac{v_z^2}{\sigma_z^2} \right]. \quad (15)$$

When the Sun is on the long axis of the ellipsoid we have the relations

$$\sigma_x^2 = \frac{v_0^2}{(2+\gamma)(p^{-2}+q^{-2}-1)}, \quad \sigma_y^2 = \frac{v_0^2(2p^{-2}-1)}{2(p^{-2}+q^{-2}-1)}, \quad \sigma_z^2 = \frac{v_0^2(2q^{-2}-1)}{2(p^{-2}+q^{-2}-1)}. \quad (16)$$

When the Sun is on the intermediate axis of the ellipsoid we have the relations

$$\sigma_x^2 = \frac{v_0^2 p^{-4}}{(2+\gamma)(1+q^{-2}-p^{-2})}, \quad \sigma_y^2 = \frac{v_0^2(2-p^{-2})}{2(1+q^{-2}-p^{-2})}, \quad \sigma_z^2 = \frac{v_0^2(2q^{-2}-p^{-2})}{2(1+q^{-2}-p^{-2})}. \quad (17)$$

Here p and q describe the axis ratios of the ellipsoid ($p = q = 1$ is a spheroid) and γ describes the anisotropy ($\gamma = 1$ for a sphere). We will consider the cases where $p = 0.9$ and $q = 0.8$ for both positions of the Sun. We will also consider $\gamma = -1.78$ (radially anisotropic) and $\gamma = 16$ (tangentially anisotropic).

4. Galactic Infall—Sikivie Caustic Model

The caustic model is based on the work of Sikivie and collaborators [14]. It is derived from the assumption that WIMPs continuously fall into our Galaxy from all directions. The WIMPs only get thermalized after many passes through the Galaxy. Thus the WIMP halo of our Galaxy should be made up of an isothermal (or similar) core plus a set of inflowing and outgoing peaks in velocity space with the distribution function given by

$$f(\mathbf{v}) = \sum_j \rho_j \delta(\mathbf{v} - \mathbf{v}_j). \quad (18)$$

Here j sums over the velocity flows, ρ_j is the density in each flow, and \mathbf{v}_j is the velocity of each flow. The peaks for one such model are given in table I. Notice that there are two flows for each velocity peak. In this model the total local density of WIMPs is $\rho_0 = 0.52 \text{ GeV/cm}^3$ and the first 14 peaks are not thermalized (Sikivie, private communications). From table I we find $\rho_{\text{caustic}} = 0.34 \text{ GeV/cm}^3$. Thus 65% of the WIMPs are in the form of velocity flows and the remaining 35% are in the form of a thermalized distribution. For simplicity we will choose the standard ($v_0 = 220 \text{ km/s}$) isothermal model for the thermalized distribution.

Most recently a number of groups have begun to numerically investigate the growth of our Galactic halo via accretion in N-body simulations. While we plan to incorporate these results into a future analysis, it is worth stressing that while the Sikivie model is undoubtedly an idealization of the actual hierarchical accretion process, the resulting distribution, containing a thermalized background plus several different unthermalized velocity flows may share some qualitative features of the N-body distribution, even if it is not likely to agree in detail with these results. It thus provides one tractable example of the complexity that might actually characterize the real galactic halo, and can usefully demonstrate some of the possible implications of phase space flows for signatures in WIMP detectors.

B. Motion of the Earth

In previous analyses it was generally assumed that the Earth orbits the Sun in the same plane that the Sun orbits the center of the Galaxy. In fact this is not true, the Earth's orbit is tilted by approximately 60° from this plane. When working with an isothermal model and considering either the total number of events or the annular modulation, the effect of the tilt of the Earth's orbit is insignificant. However, since we are interested here in angular effects and in halo models that need not be spherically symmetric, it is necessary to use the correct velocity of the Earth. In the frame of the Galaxy this is

$$\begin{aligned} v_{\oplus,x} &= 0.13v_\odot \sin(2\pi(t-t_p)/\text{year}), \\ v_{\oplus,y} &= -0.11v_\odot \cos(2\pi(t-t_p)/\text{year}), \\ v_{\oplus,z} &= v_\odot [1.05 + 0.06 \cos(2\pi(t-t_p)/\text{year})], \end{aligned} \quad (19)$$

where $v_\odot = 220 \text{ km/s}$ is the velocity of the Sun in the frame of the Galaxy, t is measured in days, and $t_p \approx 153$ days (June 2) is the day when the direction of the Earth's motion around the Sun matches the direction of the Sun's motion around the Galactic center. The numerical coefficients reflect the 60° tilt of the Earth's orbit.

The distribution functions above are given in the rest frame of the Galaxy. In the lab frame (rest frame of the Earth) we must shift them as $f(\mathbf{v} + \mathbf{v}_\oplus)$.

C. Form Factor

In WIMP-nucleus scattering, a form factor is incorporated into the cross section, as described above, to account for the loss of coherence over the nucleus for large momentum transfers. The appropriate specific form factor is, of course, nucleus-dependent. However, for the purposes of this analyses we utilize several reasonable analytical approximations which are appropriate in the case of either spin-dependent, or spin-independent scattering, as described below. For a more detailed discussion see [1].

1. Spin Independent

Here the WIMP couples to various quantum numbers of the entire nucleus. The standard form factor, $F^2(Q)$, for such nuclear interactions is the Wood-Saxon form factor. In this work we will consider the simpler exponential form factor

$$F^2(Q) = e^{-Q/Q_0} \quad (20)$$

since it is easier to work with analytically and it produces qualitatively similar results. Here $Q_0 = 3 / (2m_n r_0^2)$ and $r_0 = 0.3 + 0.91 \sqrt[3]{m_n}$ is the radius of the nucleus (in femtometers when m_n is in GeV).

2. Spin Dependent

The energy dependent component of the form factor for an axial vector interaction is given by

$$F^2(q) \propto S(q) = a_0^2 S_{00}(q) + a_1^2 S_{11}(q) + a_0 a_1 S_{01}(q). \quad (21)$$

Here a_0 (a_1) represents the isoscalar (isovector) parameterization of the matrix element. S_{00} , S_{11} , and S_{01} are obtained from detailed nuclear calculations. In this work we will parameterize this energy dependent part using exponential functions for analytical ease.

For the purposes of our calculation we choose germanium. While it is not likely that this material will in fact be used in direction-sensitive detectors, it has the virtue of being a mid-range nucleus with sensitivity to axial couplings, and has been well studied. Without specific candidates for directional detector targets it thus seems a reasonable first step, in order to get some idea of the possible changes in signature for spin-dependent vs. spin independent interactions. For germanium, we find

$$S_{\text{Ge}}(q) = 0.20313 (1.102 a_0^2 e^{-7.468y} + a_1^2 e^{-8.856y} - 2.099 a_0 a_1 e^{-8.191y}), \quad (22)$$

where $y = ((1 \text{ fm})|\mathbf{q}|/2A^{1/6})^2$ and is valid for $y < 0.2$ [15]. For a WIMP that is a pure bino the couplings are $a_0 = 0.082\zeta_q$ and $a_1 = 0.276\zeta_q$ when the European Muon Collaboration values for the spin content of the nucleons are employed. For our purposes in this work ζ_q is an energy independent, overall scale factor. See [15] for a more thorough discussion of S_{Ge} .

D. Rotating Halo

To allow for a rotating halo we employ the standard technique from Lynden-Bell [16]. Let

$$f_+(v, \alpha, \beta) = \begin{cases} f(v, \alpha, \beta) & 0 < \alpha < \pi/2 \\ 0 & \pi/2 < \alpha < \pi \end{cases} \quad (23)$$

and

$$f_-(v, \alpha, \beta) = \begin{cases} 0 & 0 < \alpha < \pi/2 \\ f(v, \alpha, \beta) & \pi/2 < \alpha < \pi \end{cases}. \quad (24)$$

Then the rotating distribution function is given by

$$f_R(v, \alpha, \beta) = (1 + \kappa)f_+(v, \alpha, \beta) + (1 - \kappa)f_-(v, \alpha, \beta). \quad (25)$$

Note that this definition does not change the normalization nor dispersion of the distribution function; $\langle f_R \rangle = \langle f \rangle$ and $\langle v^2 f_R \rangle = \langle v^2 f \rangle$, independent of κ . When $\kappa = 0$ we recover the original distribution function.

To generate a halo with a particular average velocity we note that

$$\langle v f_R \rangle = \frac{2v_0}{\sqrt{\pi}} \kappa. \quad (26)$$

Thus when $\langle v f_R \rangle = v_0$ we find that $\kappa = \sqrt{\pi}/2$.

E. Target Nucleus

As mentioned above we chose ^{73}Ge as our prototypical nuclear target. Germanium has both scalar and axial vector interactions with WIMPs, and thus serves as a good baseline for probing the dependencies in the angular distribution. Throughout, we assume that 25% of the recoil energy is in the detected channel (quenching factor of 0.25). The detector thresholds quoted below have taken this into account. Both argon and xenon have been discussed as likely targets in a TPC such as DRIFT [8]. There are experimental difficulties with using argon (it is naturally radioactive) and little is known about xenon gas (in particular its form factor). Thus we will not examine these targets in detail at this time.

Note that for our purposes the choice of ^{73}Ge as target is somewhat arbitrary. Since the normalization of the overall WIMP-nucleus scattering cross section is not relevant for our discussions, the chief distinction between choosing different target nuclei will be the kinematic dependence on WIMP mass vs target mass, and possible alterations in the spin-dependent form factor parameters. For most materials being used for dark matter detection, quenching factors generally lie in the 0.1 – 0.4 range and thus our choice of the measured Ge quenching factor is also relatively generic.

F. WIMP parameters

Throughout this work we focus on the shape of the nuclear recoil distribution. Thus, as emphasized above, we do not focus on the overall event rate normalization. This quantity depends on specifics of the halo density, the WIMP mass and couplings, the target nucleus, detector size, type of interaction, *etc.* The key point is that when modeling a specific detector this normalization will be essential, but in order to explore generic features of the angular signature of WIMP-nucleus scattering, it is not important.

As noted above, the mass of the WIMP affects both the normalization and shape of the nuclear recoil distribution. Thus, the results remain identical if one appropriately scales both target nucleus and WIMP mass. In this work we will consider $m_\chi = 60$ GeV as our standard WIMP mass (as mass matches well with the germanium target, $m_{\text{Ge}} = 73$ GeV). In some cases we will also show results for $m_\chi = 180$ GeV to show how the mass of the WIMP affects the results. The results we present should thus be considered to be appropriate to a WIMP whose mass matches well with the target nucleus mass, or in some cases greatly exceeds it.

IV. RESULTS

The calculations of $dR/d\Omega$ were performed on a 40×40 grid in the $(\cos \gamma, \phi)$ plane. They were calculated in 5 day bins and summed over the year. By summing over the year we average out any annual modulations in both the signal and the background. Furthermore, we are implicitly averaging over the day in which time the detector rotates (along with the Earth) by 2π with respect to the direction of motion. Thus any angular dependent backgrounds, due to, for example, hot spots in the detector, will also be averaged out (at least for the component in the plane of motion of the Earth) and the probability of a background induced nuclear recoil is uniform in angle when averaged over the year, with respect to the direction of the Earth's motion around the Sun.

A. Angular Distributions

The angular distribution for the isothermal model with $v_0 = 220$ km/s is shown in figure 2. Notice the exponential decay in $\cos \gamma$ in the forward direction and the independence of ϕ . The reason for the decay in the forward direction is simple. The Earth is moving through this WIMP halo, and thus more WIMPs are incident from the forward direction

than the backward direction, and thus nuclei are preferentially scattered backwards. This exponential decay would lead to an easy statistical separation of signal events from (flat) background events as discussed below. To examine dependence on threshold we plot $dR/d\Omega$ for $\phi = 0$ for a number of different threshold energies (figure 3). As we increase the threshold the backward scattering peak in the distribution becomes more pronounced in relation to the rest of the distribution, making it more easily distinguishable from a (flat) background. However, as is also evident from the figure, as we increase the threshold the total number of events decreases. These two effects will be discussed below.

The angular distributions for a number of isothermal, axisymmetric and rotating models are shown in figure 4. Here we plot $dR/d\Omega$ as a function of $\cos\gamma$ for $\phi = 0$ and $E_{\text{th}} = 0$ keV. The two solid curves for the $v_0 = 220$ km/s isothermal model are for two different WIMP masses, $m_\chi = 60$ GeV and $m_\chi = 180$ GeV. All of the curves are normalized so that $R = 1$. As can be seen from the figure all of the models are similar in shape (at least at $E_{\text{th}} = 0$ keV). Thus we do not expect a large variation in the number of events required to identify a WIMP signal as we will discuss later. On the other hand, it also means that it will be difficult to distinguish between different halo models based solely on this information.

The angular distribution for the triaxial model is shown in figure 5. Here there is a panel for each set of parameters. This shows how much the rate can vary even in a single model depending on the parameters. The most difficult combination of parameters to distinguish from background is seen in panel (a) since it looks the most similar to a flat distribution. The rest of the models look more like the isothermal distribution (panels b–d) and will be easier to distinguish from the background.

The angular distribution for the caustic model is shown in figure 6. Here both the pure caustic and a caustic with isothermal component are shown. Notice that the pure caustic model is peaked in the forward direction (opposite the other models) and falls off more slowly. This is because we are located near a caustic and WIMPs are preferentially catching up with the Sun as it moves through the Galaxy, so more are incident from behind than from the forward direction. There are also a number of small features in the ϕ direction. When combined with the $v_0 = 220$ km/s isothermal model the distribution flattens greatly. This makes it more difficult to distinguish from a flat background than the other models.

B. Signal Identification

To determine the number of signal events necessary to identify a WIMP signal we employ a maximum likelihood analysis along with Monte Carlo generation of sample nuclear recoil distributions. We define a likelihood function

$$\mathcal{L} = \prod_{i=1}^{N_e} P(\cos\gamma_i, \phi_i), \quad (27)$$

where N_e is the total number of events and $P(\cos\gamma_i, \phi_i)$ is the probability of nuclear recoil in the (γ_i, ϕ_i) direction for a particular model (e.g. an isothermal model). Here $P(\cos\gamma_i, \phi_i)$ is generated by calculating $dR/d\Omega$ for each recoil direction (γ_i, ϕ_i) and averaging the result over the year in 5 day bins. At the 95% confidence level when $\log \mathcal{L}_{dR/d\Omega} - \log \mathcal{L}_{\text{flat}} < 1$ the distributions are indistinguishable. We generate 10,000 data sets for each N_e and demand that the log-likelihood condition is satisfied less than 5% of the time. The smallest N_e for which this occurs is the minimum number of events required to get a 95% detection 95% of the time.

With this procedure we can determine the number of events required to distinguish a signal from a flat background or to distinguish one signal (e.g. an isothermal halo) from another signal (e.g. a caustic halo). For a pure signal we use $P_{dR/d\Omega}$ as determined by the shape of $dR/d\Omega$. For a signal-to-noise ratio, S/N , we replace P with $P_{\text{total}} = \lambda P_{\text{flat}} + (1 - \lambda)P_{dR/d\Omega}$ where $\lambda = 1/(1 + S/N)$. For the results discussed here we consider a 40×40 grid in the $(\cos\gamma, \phi)$ plane and assume perfect angular knowledge on this grid. This implies an accurate angular recoil detector. We also consider the case where knowledge of just the forward-backward asymmetry is available. In this case P is replaced by a binomial distribution.

In figure 7 we show the number of signal events needed to differentiate a WIMP signal from a flat background at the 95% confidence level 95% of the time for a standard isothermal halo. In this figure there are two sets of curves shown. The lower set contains the results for a pure signal (no noise). The upper set contains the results for a signal to noise ratio of one, thus twice as many events as shown would have been detected (roughly half signal and half noise). In each set two curves are shown. The lower curve in each set shows the actual number of events required to distinguish the WIMP signal. For the $S/N=1$ case this decreases from 32 events at $E_{\text{th}} = 0$ keV to 8 events at $E_{\text{th}} = 25$ keV. As mentioned above, this is due to the fact that the distribution becomes more peaked in the backward direction, thus it is more easily distinguished from a flat distribution. However, as also mentioned above, at a higher threshold

energy there are fewer events. Thus, for a fixed-size detector raising the threshold will not in general aid in signal detection, because most of the signal events will be discarded. We attempt to account for this fact in the upper curve in each set. The upper curve gives the number of events that would have been detected at zero threshold in order to observe the number of events shown in the lower curve for finite thresholds. This curve shows the effect of the decrease in the rate as the threshold is increased. For isothermal halos, at least, it is desirable to choose the lowest possible threshold of the detector for a fixed signal-to-noise ratio in order to improve the ability to detect WIMPs with the fewest number of events.

The effect of changing the width of the isothermal distribution (changing v_0) is shown in figure 8. As expected from figure 4 at low thresholds the narrower distribution ($v_0 = 150$ km/s) is more easily distinguished from a flat background than the broader distributions. At higher thresholds the tail of the WIMP distribution becomes important since the number of high energy nuclear recoils falls off more rapidly for narrower distributions. Note that it is still the case that the number of events required for detection is an increasing function of energy.

The number of events required for the axisymmetric isothermal models are shown in figure 9. For reference the $v_0 = 220$ km/s isothermal model is also included (solid line). Both the $q = 1$ and $q = 0.85$ models are very similar to the $v_0 = 220$ km/s isothermal model. The $q = 1/\sqrt{2}$ (maximal flattening) model is very similar to the $v_0 = 150$ km/s isothermal model.

In order to explore the general effects of spin-dependence, WIMP mass, and rotation, we display in figure 10 the predicted event distributions for a $v_0 = 220$ km/s isothermal model, while allowing these other parameters to vary. From the figure we see that the spin interaction using the form factor presented earlier leads to a steeper rise in the number of events. This is due to the steeper fall off of the spin-dependent form factor with energy compared to the spin independent form factor, and will thus be nucleus-dependent. A larger mass WIMP leads to more energy transferred to the nucleus, thus the $m_\chi = 180$ GeV WIMP requires fewer events at high threshold than the lighter $m_\chi = 60$ GeV WIMP does. A (net) corotating halo is more difficult to distinguish than the isothermal sphere as expected. However, it is not as difficult as might be expected since we have cut out some, but not all, of the WIMPs from the forward direction. This shows up more strongly as the threshold is increased.

It is important to note that all of the above distributions require roughly the same number of events in order to distinguish a signal from a flat background. If this were generic, then low-threshold detectors sensitive to roughly 30-50 events would be guaranteed to unambiguously identify a WIMP signal, even if a distinction between halo models might not be easy. Unfortunately, however, two of the models we have considered here, both of which exist in the literature as candidates for our Galactic halo, will require far more events in order to disentangle the signal from a flat background. For the reasons mentioned earlier, it is reasonable to expect that the distributions that arise from N-body simulations may share these features.

First, we consider the caustic distribution. As is expected from figure 6, this most closely resembles a flat distribution and thus requires the most number of events. Also not surprisingly it is a strong function of threshold energy. As the threshold is increased some of the velocity peaks do not contribute detectable nuclear recoils thus greatly changing the shape of the recoil distribution. We note that the number of events required for detection is not a monotonic function. Thus the detection of WIMPs in a caustic halo will depend sensitively on the mass of the WIMP and the threshold of the detector. A range of thresholds would need to be probed. In practice also having energy information about the event will most likely prove to be extremely important to differentiate WIMP events from background events in this case.

Next we consider the triaxial logarithmic ellipsoidal model. As expected from figure 5 most of the models are not too different from the standard isothermal sphere 11. However, when the Sun is on the intermediate axis and we have a radial anisotropy ($\gamma = -1.78$) approximately 120–150 events are required. This model shows the importance of exploring a broad class of halos and parameters in order to assess the requirements of a a detector with angular resolution.

In the above results we have assumed fairly accurate angular resolution (bins of about 9 degrees in width were used). However a real detector may not be able to achieve this level of angular resolution. To explore this we consider the case of only having knowledge of the forward to backward asymmetry. In this case the events fall into one of two bins. In our likelihood analysis we compare two binomial distributions; one for the data with fraction of events in the forward bin as our probability and the other for the flat background where the probability is a half.

In figure 12 we show the number of signal events needed to differentiate a WIMP signal from a flat background at the 95% confidence level 95% of the time when only two angular bins are employed (forward and backward). This figure is the counterpart of figure 7. Even in this case of relatively little angular information few events are needed. For $S/N = 1$ if $E_{th} < 5$ keV then $N_{events} \approx 40-65$. It is interesting to note that thresholds slightly above zero give a somewhat more discernible signal in this case.

The results for the other models considered in this work are shown in figures 13–16. These figures should be compared to figures 8–11. In most cases we see the slight dip (or at least very slow rise) in the number of events

needed around $E_{\text{th}} \approx 2$ keV. We note that the result for the caustic model is not shown. As previously mentioned the caustic model most closely resembles a flat distribution. This shows up most prominently here where we have limited the angular information available. In this case the number of events needed with $S/N = 1$ at $E_{\text{th}} = 0$ keV is about 5200. Again most of the triaxial models are not that different than the isothermal sphere. However the radially anisotropic model with the Sun on the intermediate axis again requires the most number of events. Here approximately 250–300 events are required for $E_{\text{th}} < 5$ keV.

The DRIFT detector in its current form will only obtain information about the recoil in two directions. One will be along the axis of the Sun’s motion through the Galaxy (z -axis in our coordinates) and the other either the x or y -axis. Having information along the z -axis is necessary to have any ability to identify WIMPs. Since the recoil distribution is essentially independent of ϕ (or equivalently the x, y -plane, see figure 7) having information on these two axes is almost the same as having the full angular distribution. We have calculated the number of events required to identify a WIMP signature in this case and the results are identical to those discussed above for the isothermal and axisymmetric models. Naturally in the case of the caustic model more events are required since this model has structure in the x, y -plane.

This simple study of the DRIFT’s capabilities assumed that we could identify the recoil tracks regardless of their orientation. In practice if we do not have full angular resolution then some tracks will not be resolved. For example, if we are projecting out the x -axis any event that has a large component along the x -axis and a small component along the y -axis will appear as a short track and will thus be difficult to identify. To accurately model DRIFT it would be necessary to take this track identification into account along with other detector characteristics (threshold, etc.) Furthermore it may not be possible to measure the direction of the track, only its axis. In a detector such as DRIFT that relies on ionization to measure the recoil direction, it is difficult to tell where a track begins and ends. To make this distinction we must rely on the ionization (energy deposition) as a function of the energy of the recoiling nucleus. The extent to which this can be used to determine directionality will be crucial for determining the ability of a detector to identify a WIMP signal. We will consider these details in future work.

V. CONCLUSIONS

Our results are useful when considering the construction of the next generation of WIMP detectors sensitive to the angular distribution of WIMP scattering events. As we have described, this sensitivity will provide, in principle, a key extra signature needed to unambiguously demonstrate that an observed signal is indeed WIMP-related, and one which will require both far fewer events and also be subject to fewer systematic uncertainties than exist in a search for simple annual modulations.

The formalism we have developed allows one to calculate the angular distribution of recoil events, $dR/d\Omega$, and the distribution in both energy and angle, $d^2R/dQd\Omega$. This formalism accommodates arbitrary velocity space WIMP distributions and correctly employs the full motion of the Earth around the Sun and the Sun through the Galaxy. As such, it can be used as an input to any detector Monte Carlo, allowing a determination of the predicted angular distribution of events for any halo model.

While we hope to utilize our analysis to examine various specific detectors possibilities in the future, we have thus far derived various generic predictions for the range of events that will be required in an idealized detector, given our present uncertainty in the actual Galactic halo WIMP distribution. We feel this is an important first step in order to set the scale of detector parameters that may be required to adequately exploit angular sensitivity.

In particular, we have calculated the recoil distribution from WIMP scattering and the expected number of events necessary to distinguish a WIMP signal from a background with a 95% confidence level for various analytic halo models; isothermal models with $v_0 = 150$ km/s, 220 km/s, and 300 km/s; Evans models with flattening $q = 1, 0.85,$ and $1/\sqrt{2}$, and rotating halo models. In all such cases the number of events required is quite low, typically 50–70 for $E_{\text{th}} < 5$ keV when the full angular distribution is measured. Even if only the forward to backward ratio is measured relatively few events are required, typically 70–110 for $E_{\text{th}} < 5$ keV for these models. This study considered WIMPs with masses $m_\chi = 60$ GeV and 180 GeV and included both spin dependent and independent interactions. We note that spin-dependent interactions may require lower thresholds in order to have sufficient number of events to distinguish a WIMP signal.

The isothermal and Evans models are both axisymmetric. As extreme asymmetric models we also studied the case of caustics (peaks) in the velocity distribution, and a set of triaxial halo models. The former distribution should be considered a first pass at considering more realistic halo distributions arising from hierarchical accretion in N-body simulations. In this case the resulting recoil spectrum is very similar to a flat background and thus is rather difficult to distinguish. Here the number of events required ranges from 300–600 for $E_{\text{th}} = 2$ –10 keV and depends rather sensitively on the threshold. For the triaxial model most sets of parameters lead to limits similar to the isothermal

sphere. Only the case of the Sun on the intermediate axis with a radial anisotropy ($\gamma = -1.78$) are the requirements raised to 120–150 events for $E_{\text{th}} < 5$ keV.

We have also performed a preliminary study of a DRIFT-like detector. Here we projected out one of the directions perpendicular to the direction of motion of the Sun since DRIFT will only have resolution in two directions. Here we found that the results can be as robust as having full angular resolution for axisymmetric halo models.

In future work we plan to refine our analysis in several ways. First, we will exploit the output of existing N-body simulations to explore the consequences for the expected angular signals. Next, we plan to carry out an analysis similar to the present analysis for specific proposed detectors. This will allow us to explore the very important issue of utilizing energy as well as angular sensitivity, but it will also require us to adequately model the expected energy dependence of various detector backgrounds. Finally, after completing these analyses, we hope to explore exactly how many events may be needed to distinguish between halo models, in order to determine how an eventual WIMP detection may shed light on the unknown features of our Galactic halo, and thus on important issues associated with galaxy formation and evolution.

If a WIMP signal is ultimately observed in terrestrial detectors it will provide one of the most important observations that has ever been made in particle physics and cosmology. It is thus worthwhile considering in advance not only how one might best unambiguously disentangle such a signal from backgrounds, but also how one might then use this signal as a probe of astrophysics. Our results provide a useful first step in this direction.

We thank P. Sikivie, J. Martoff, and B. Moore for useful discussions about their research results, and J. Heo for his contributions to our initial investigations.

-
- [1] G. Jungman, M. Kamionkowski, and K. Greist, *Phys. Rep.* **267**, 195 (1996).
 - [2] R. Abusaidi, *etal.* (CDMS collaboration), *Phys. Rev. Lett.* **84**, 5699 (2000).
 - [3] Proceedings, Third International Conference on the Identification of Dark Matter, York, England, ed. N. Spooner et al., World Scientific, to appear.
 - [4] R. Bernabei, *etal.*, *Phys. Lett. B* **480**, 23 (2000).
 - [5] A.K. Drukier, K. Freese, and D.N. Spergel, *Phys. Rev.* **D33** 3495 (1986).
 - [6] D.N. Spergel, *Phys. Rev.* **D37**, 1353 (1988).
 - [7] C.J. Martoff, *etal.*, *Phys. Rev. Lett.* **76**, 4882 (1996).
 - [8] D.P. Snowden-Ifft, C.J. Martoff, and J.M. Burwell, *Phys. Rev. Lett.*, submitted, astro-ph/9904064 (1999); M.J. Lehner, *etal.*, astro-ph/9905074 (1999).
 - [9] C.J. Copi, J. Heo, and L.M. Krauss, *Phys. Lett. B* **461**, 43 (1999).
 - [10] P.F. Smith and J.D. Lewin, *Phys. Rep.* **187** 203 (1990).
 - [11] N.W. Evans, *Mon. Not. R. Astron. Soc.* **260**, 191 (1993).
 - [12] M. Kamionkowski and A. Kinkhabwala, *Phys. Rev.* **D57**, 3256 (1998).
 - [13] N.W. Evans, C.M. Carollo, and P.T. de Zeeuw, astro-ph/0008156 (2000).
 - [14] P. Sikivie, I.I. Tkachev, and Y. Wang, *Phys. Rev.* **D56**, 1863 (1997).
 - [15] M. Ted Ressel, *etal.*, *Phys. Rev.* **D48**, 5519 (1993).
 - [16] D. Lynden-Bell, *MNRAS* **136**, 101 (1967).

TABLE I. Velocity flows of dark matter from the Caustic model (for $h = 0.75$, $\epsilon = 0.28$, $j_{\max} = 0.25$ Sikivie model (Sikivie, private communications)). Velocities are given in the rest frame of the Galaxy.

Flow	ρ^a	v_x^b	v_y^b	v_z^b
1	0.4	140	0	± 600
2	0.9	250	0	± 500
3	2.0	350	0	± 395
4	6.1	440	0	± 240
5	9.6	440	± 190	0
6	3.0	355	± 290	0
7	1.9	295	± 330	0
8	1.4	250	± 350	0
9	1.0	215	± 355	0
10	1.1	190	± 355	0
11	0.9	170	± 355	0
12	0.8	150	± 350	0
13	0.7	135	± 345	0
14	0.6	120	± 340	0

^aIn units of 10^{-26} g/cm³.

^bIn units of km/s.

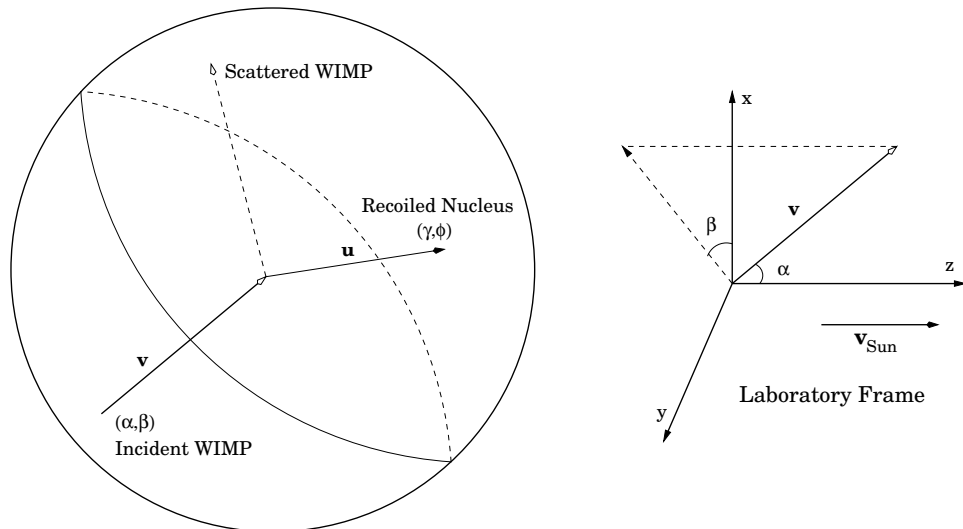


FIG. 1. Geometry of a WIMP scattering event. Here a WIMP is incident at an angle (α, β) in the lab frame (shown on the right). The WIMP hits a nucleus originally at rest that recoils at an angle (γ, ϕ) in the lab frame. The velocity of the Sun through the Galaxy defines the z -axis in the laboratory frame.

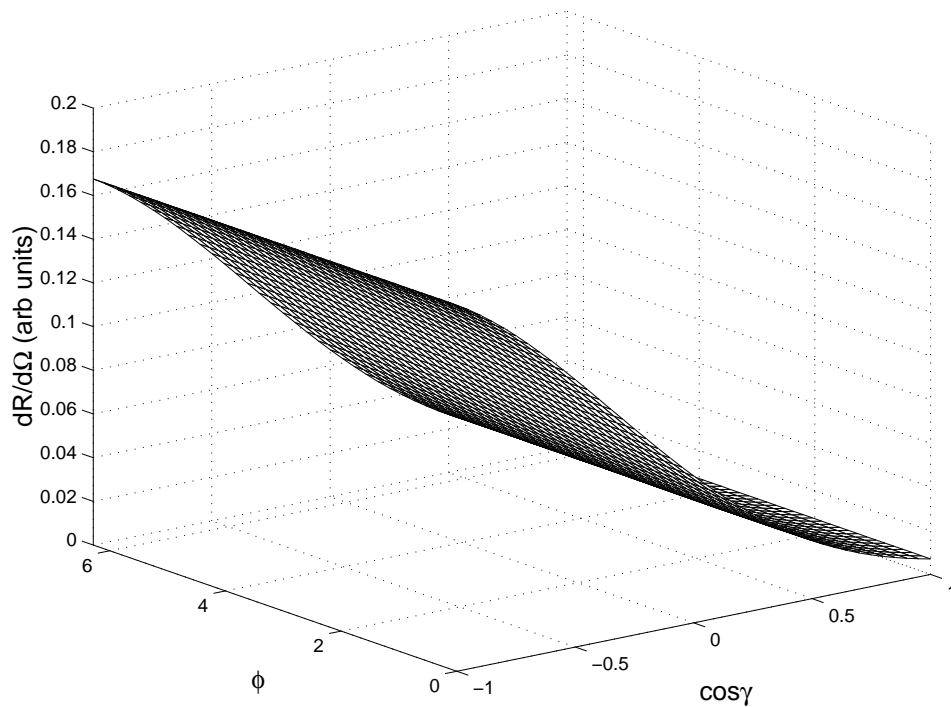


FIG. 2. The angular distribution of nuclear recoil events, $dR/d\Omega$ for an isothermal halo model. Here $v_0 = 220$ km/s and $E_{\text{th}} = 0$ keV.

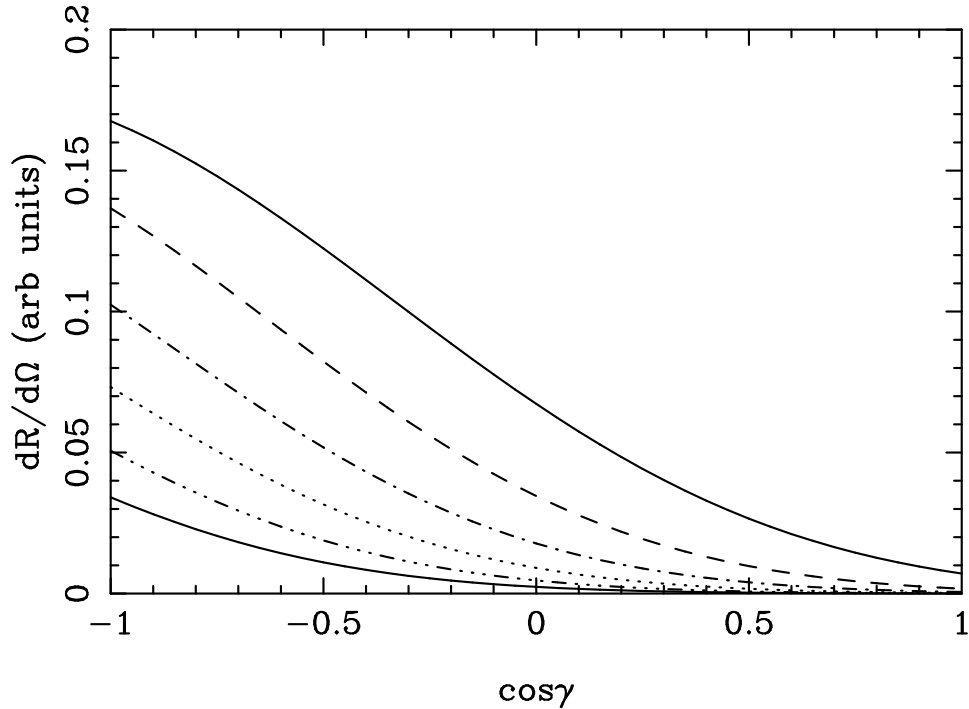


FIG. 3. The angular distribution of nuclear recoil events, $dR/d\Omega$ for an isothermal halo model with $\phi = 0$ and $v_0 = 220$ km/s as a function of $\cos \gamma$ and for various threshold energies. Here the thresholds are (from upper to lower) $E_{\text{th}} = 0$ keV (upper solid curve), 2 keV, 4 keV, 6 keV, 8 keV, and 10 keV (lower solid curve).

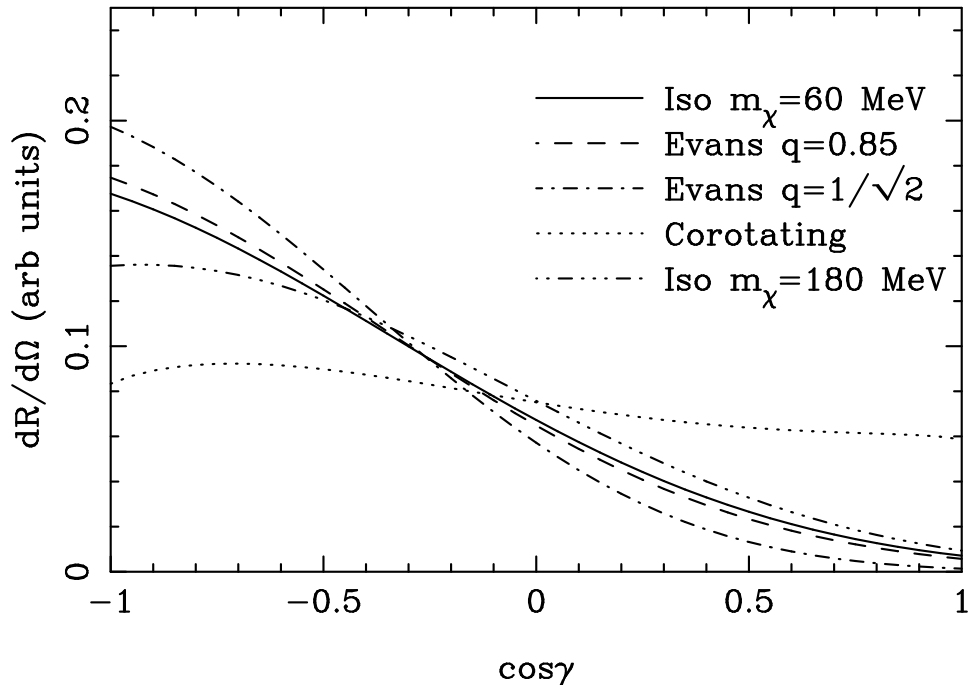


FIG. 4. The angular distribution of nuclear recoil events, $dR/d\Omega$ for the isothermal and Evans halo models with $\phi = 0$ $E_{\text{th}} = 0$ keV as a function of $\cos \gamma$. The Evans model with $q = 1$ is not shown since it is nearly identical to the isothermal model with $v_0 = 220$ km/s. There are two curves shown for the $v_0 = 220$ km/s isothermal model; one for $m_\chi = 60$ GeV (solid line) and the other for $m_\chi = 180$ GeV (dashed-dotted line). The Evans model with $q = 0.85$ (dashed line) and $q = 1/\sqrt{2}$ (long dashed-short dashed line) are also shown. Finally the corotating model (dotted line) is shown. See the text for more details.

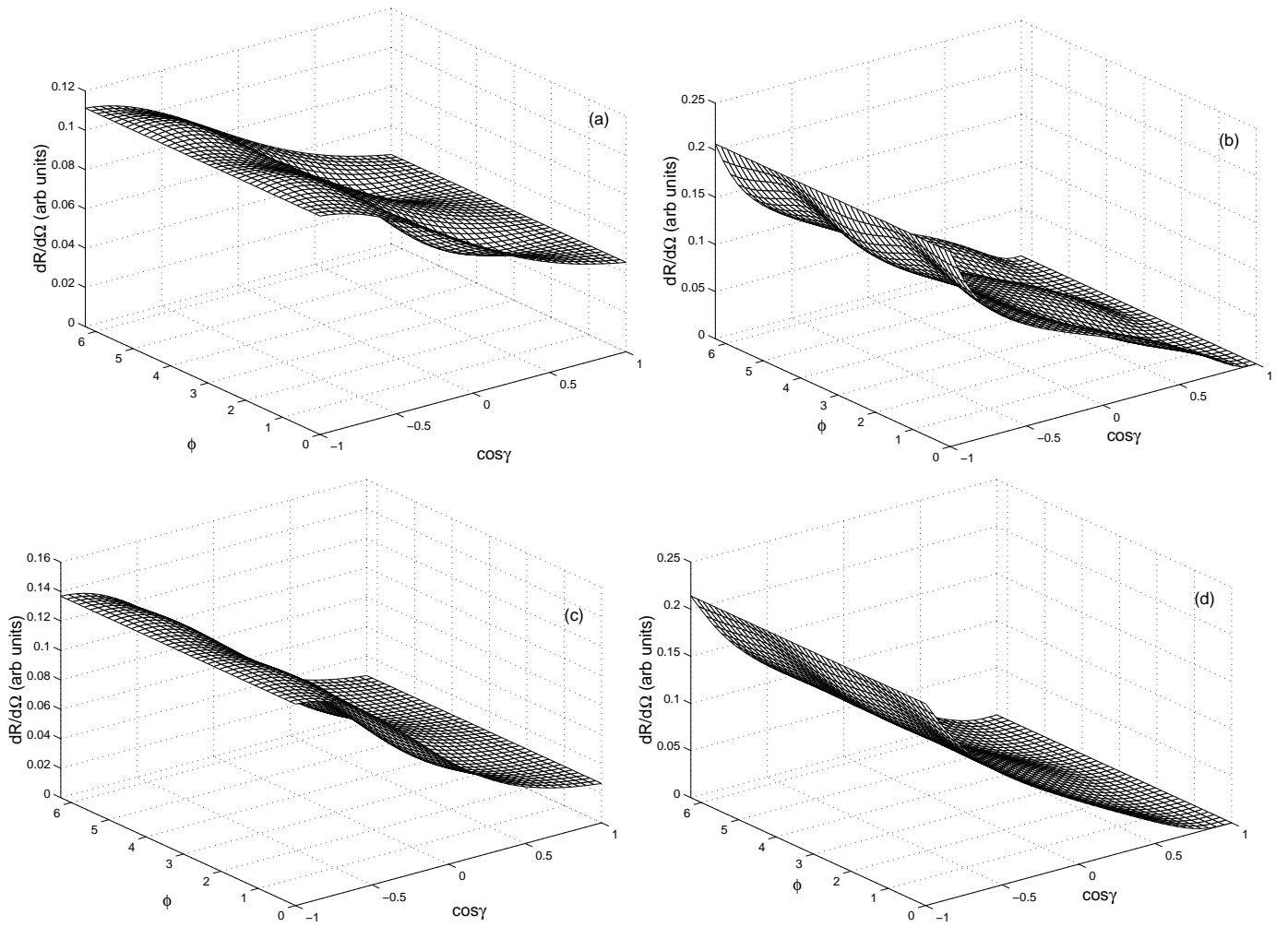


FIG. 5. The angular distribution of nuclear recoil events, $dR/d\Omega$ for the triaxial model for $E_{\text{th}} = 0$ keV. In all cases $p = 0.9$ and $q = 0.8$. We consider the Sun on the intermediate axis (a) $\gamma = -1.78$ (radially anisotropic) and (b) $\gamma = 16$ (tangentially anisotropic). We also consider the Sun on the major axis (c) $\gamma = -1.78$ (radially anisotropic) and (d) $\gamma = 16$ (tangentially anisotropic).

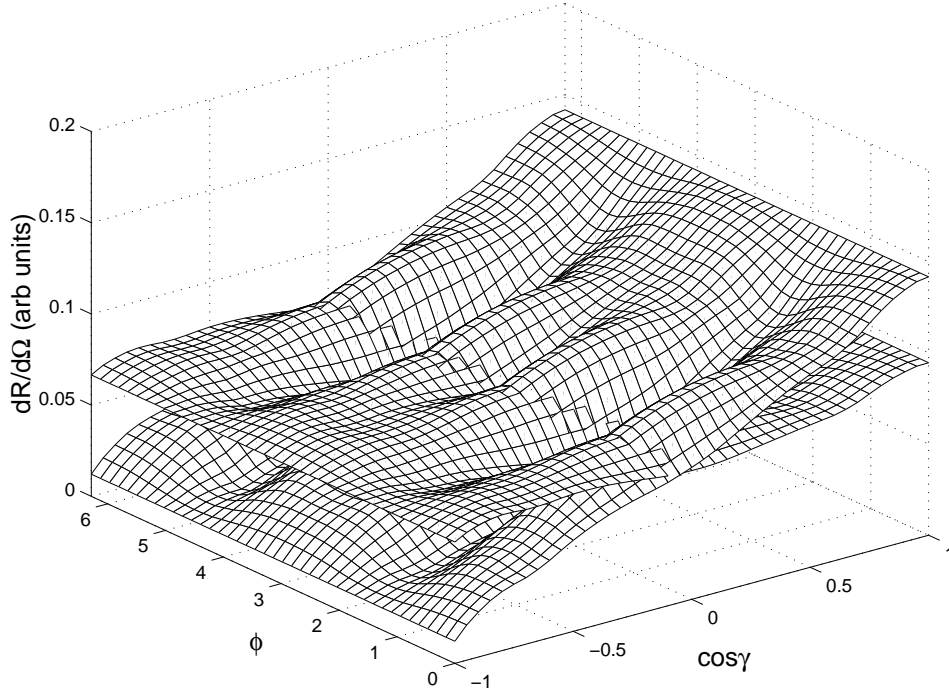


FIG. 6. The angular distribution of nuclear recoil events, $dR/d\Omega$ for the caustic model. Here the contribution from the caustics (steeper) and the actual caustic plus $v_0 = 220$ km/s isothermal (flatter) distributions are shown for $E_{\text{th}} = 0$ keV.

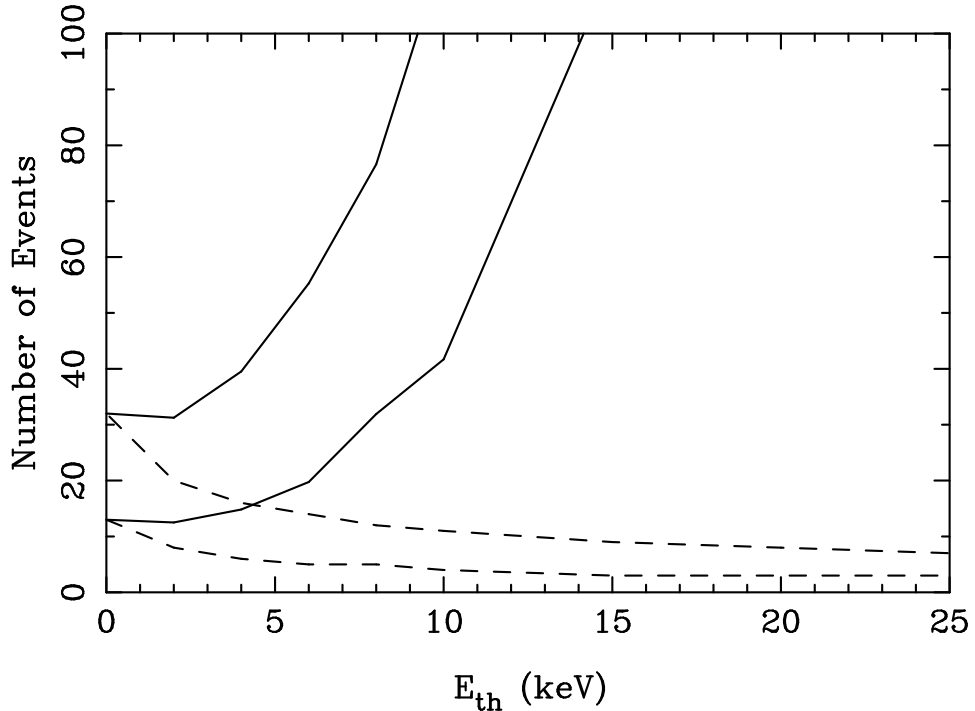


FIG. 7. The number of signal events required as a function of threshold energy to distinguish an isothermal distribution of WIMPs in the halo with $v_0 = 220$ km/s from a flat background. The bottom set of curves is for a pure signal and the top set of curves is for a signal-to-noise ratio of 1. The dashed curves show the number of events needed as a function of threshold energy. The solid curves show the number of events needed for $E_{\text{th}} = 0$ keV in order to achieve the necessary number of events at the higher thresholds. These curves include the fact that the number of events detected falls quickly as the threshold is increased. See the text for more details.

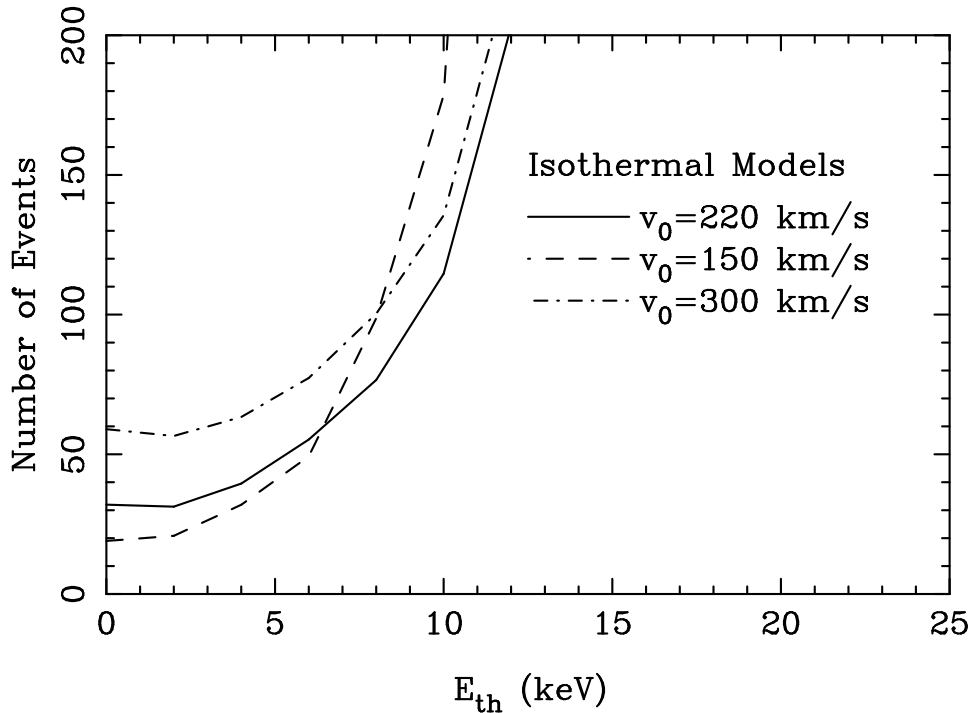


FIG. 8. The number of signal events required as a function of threshold energy to distinguish an isothermal distribution of WIMPs in the halo from a flat background. Here we have considered three values for the dispersion in the halo, $v_0 = 220$ km/s (solid line), $v_0 = 150$ km/s (dashed line), and $v_0 = 300$ km/s (long dashed-short dashed line). See the text for a discussion.

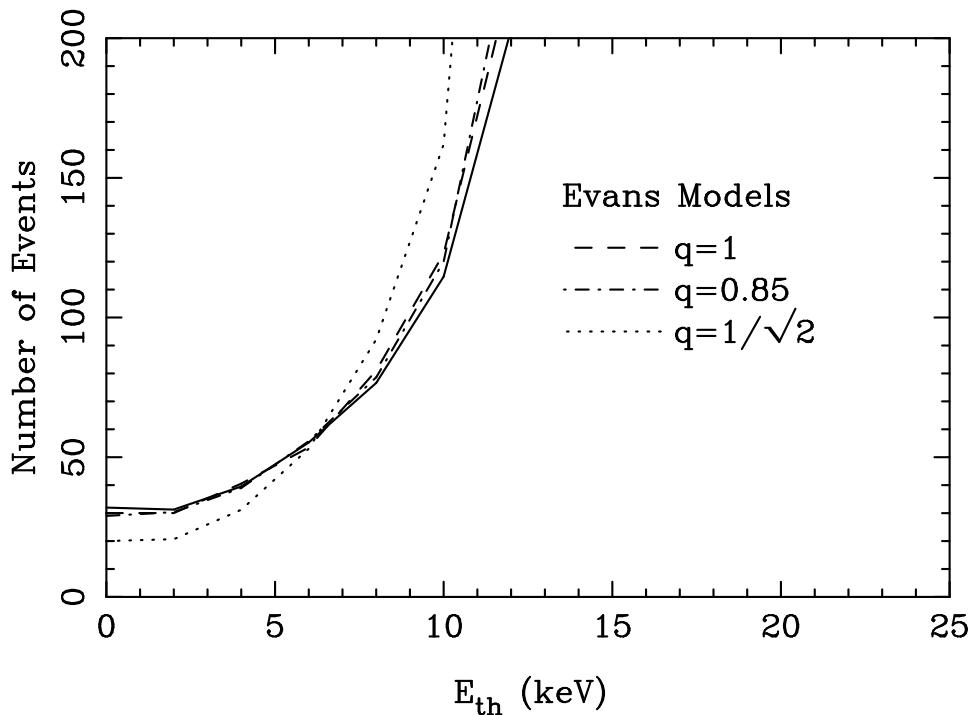


FIG. 9. The number of signal events required as a function of threshold energy to distinguish WIMPs in the halo distributed according to an Evans model from a flat background. Here we have considered three values for the flattening of the halo, $q = 1$ (dashed line), $q = 0.85$ (long dashed-short dashed line), and $q = 1/\sqrt{2}$ (dotted line). The standard $v_0 = 220$ km/s isothermal model (solid line) is shown for reference. See the text for a discussion.

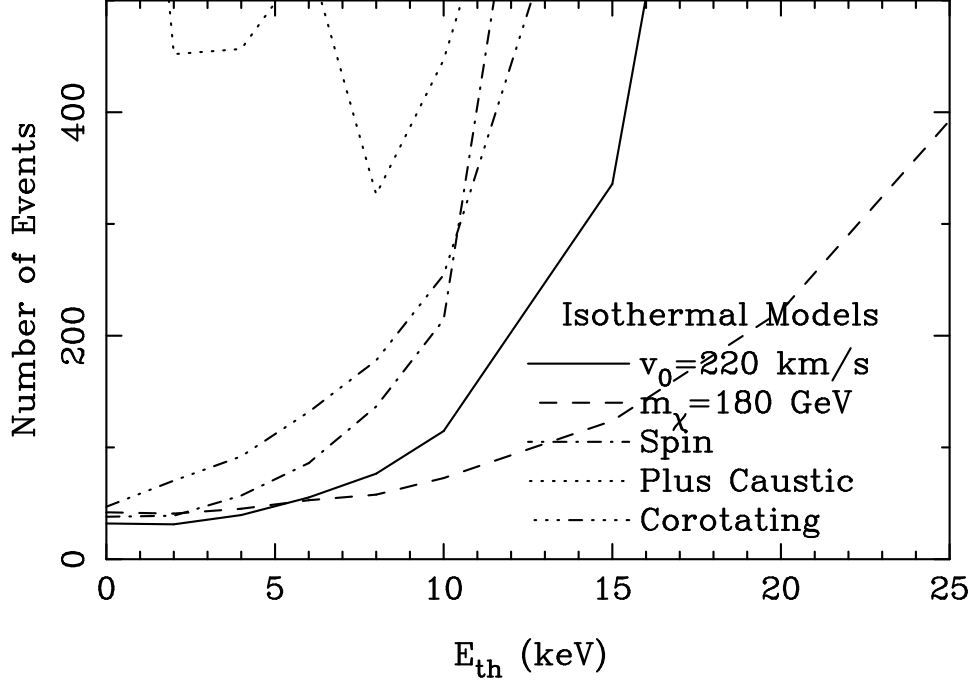


FIG. 10. The number of signal events required as a function of threshold energy to distinguish various isothermal distributions of WIMPs in the halo from a flat background. Here we have considered a WIMP of mass $m_\chi = 180$ GeV (dashed line), the spin dependent (axial vector) interaction (long dashed-short dashed line), the caustic model (with an isothermal component, dotted line), and a corotating model (dashed-dotted line). The standard $v_0 = 220$ km/s isothermal model (solid line) is shown for reference. See the text for a discussion.

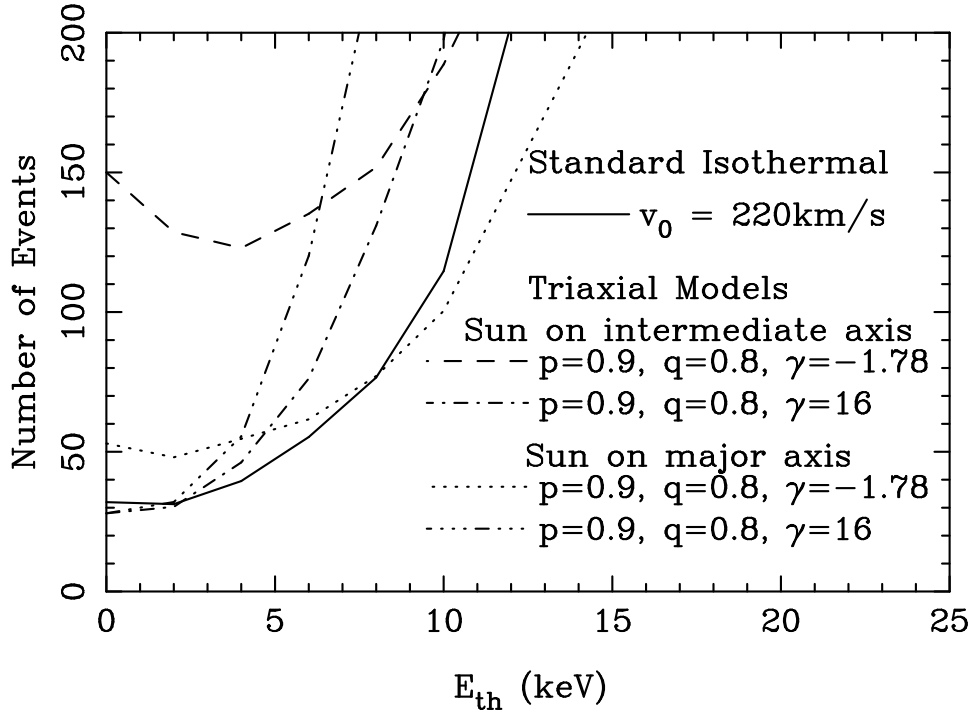


FIG. 11. The number of signal events required as a function of threshold energy to distinguish a triaxial distribution of WIMPs in the halo from a flat background. Here we have considered a the Sun on the intermediate axis with $\gamma = -1.78$ (dashed line) and $\gamma = 16$ (long dashed-short dashed line) and the Sun on the major axis with $\gamma = -1.78$ (dotted line) and $\gamma = 16$ (dashed-dotted line). The standard $v_0 = 220$ km/s isothermal model (solid line) is shown for reference. See the text for a discussion.

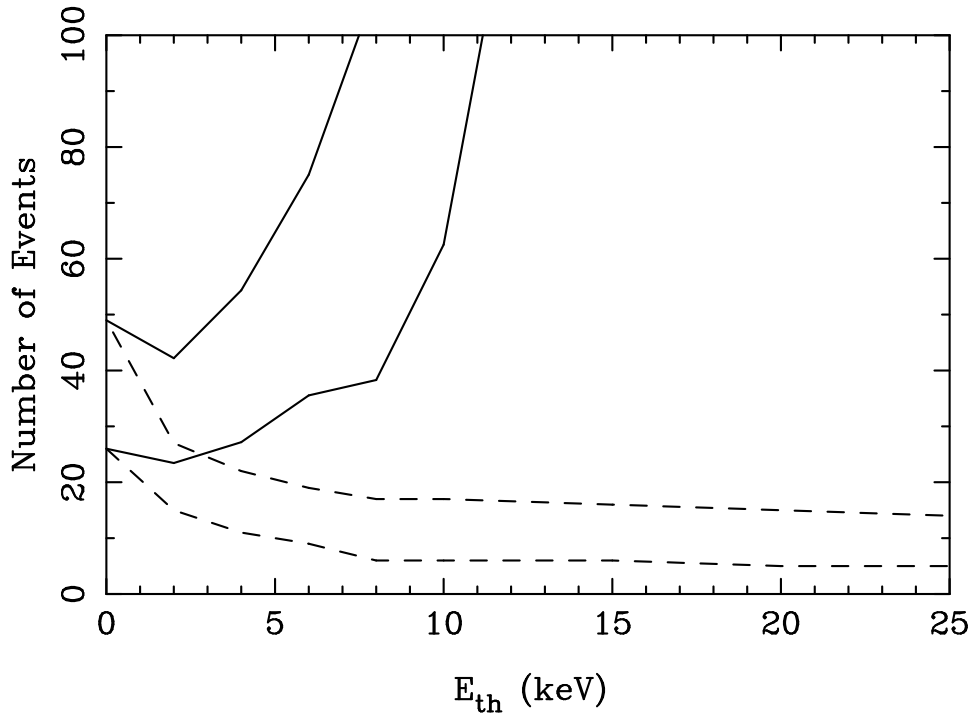


FIG. 12. The number of signal events required as a function of threshold energy to distinguish an isothermal distribution of WIMPs in the halo with $v_0 = 220$ km/s from a flat background using only the forward to backward ratio. See figure 7 and the text for more details.

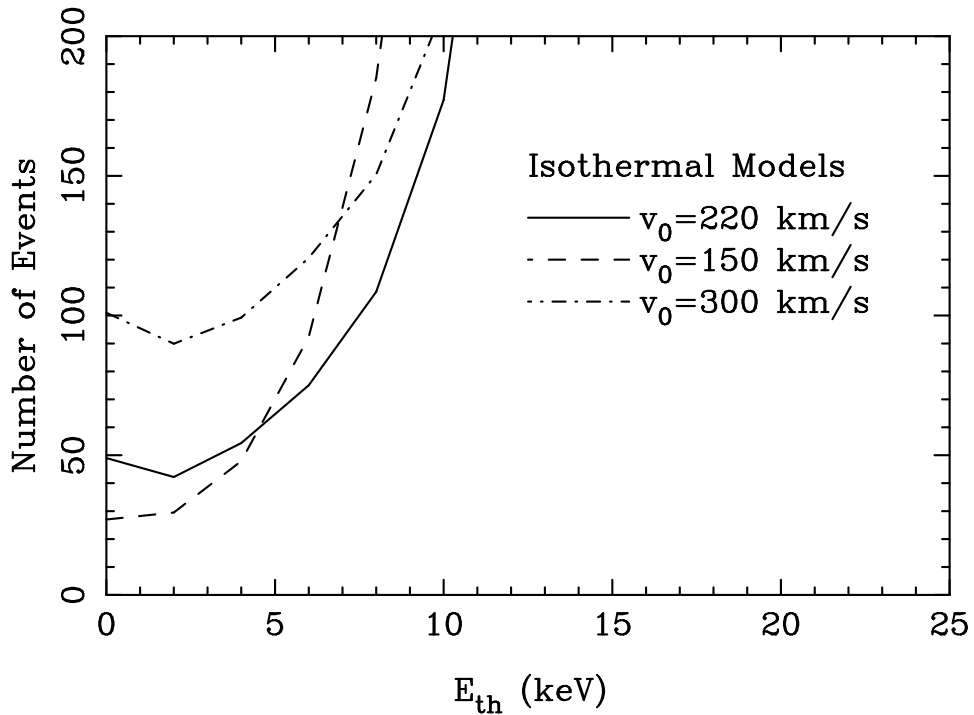


FIG. 13. The number of signal events required as a function of threshold energy to distinguish an isothermal distribution of WIMPs in the halo from a flat background using only the forward to backward ratio. Here we have considered three values for the dispersion in the halo, $v_0 = 220$ km/s (solid line), $v_0 = 150$ km/s (dashed line), and $v_0 = 300$ km/s (long dashed-short dashed line). See figure 8 and the text for more details.

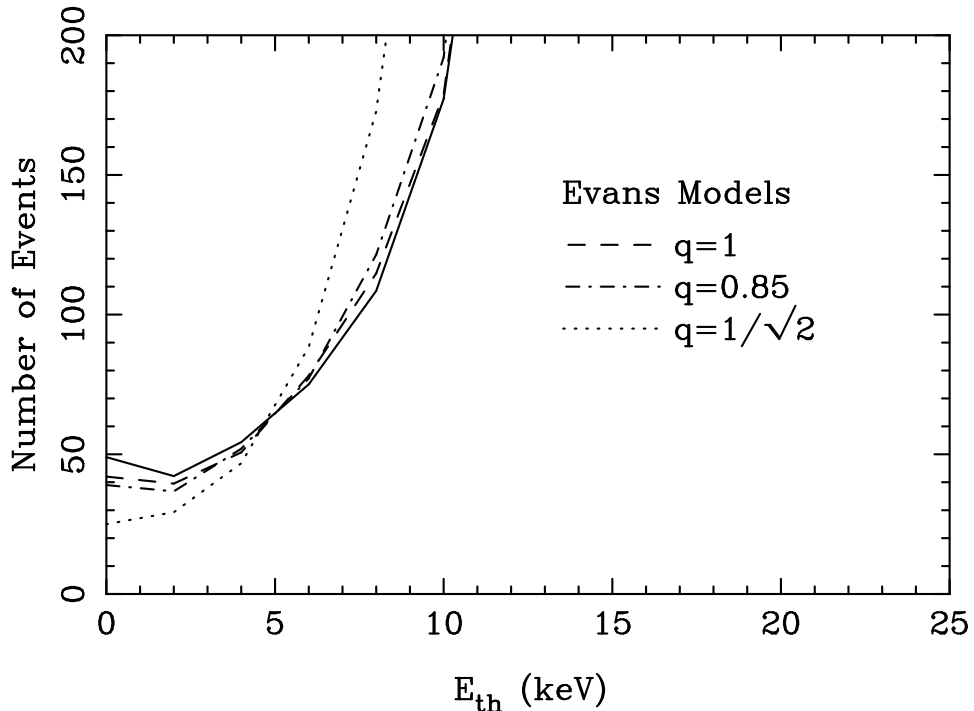


FIG. 14. The number of signal events required as a function of threshold energy to distinguish WIMPs in the halo distributed according to an Evans model from a flat background using only the forward to backward ratio. Here we have considered three values for the flattening of the halo, $q = 1$ (dashed line), $q = 0.85$ (long dashed-short dashed line), and $q = 1/\sqrt{2}$ (dotted line). The standard $v_0 = 220$ km/s isothermal model (solid line) is shown for reference. See figure 9 and the text for more details.

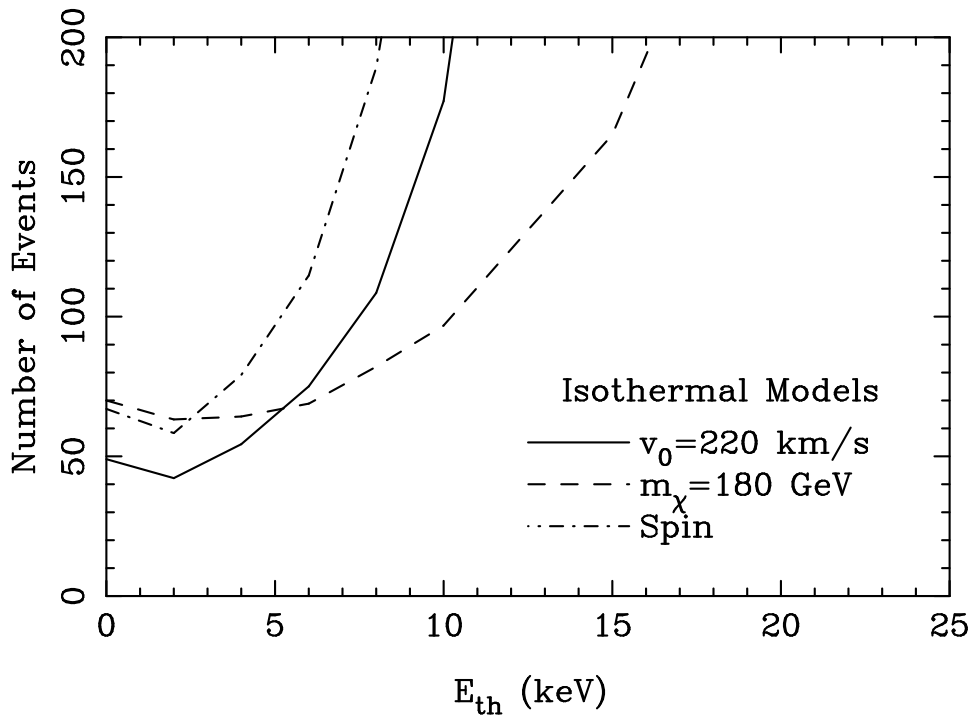


FIG. 15. The number of signal events required as a function of threshold energy to distinguish various isothermal distributions of WIMPs in the halo from a flat background using only the forward to backward ratio. Here we have considered three values for the flattening of the halo, $q = 1$ (dashed line), $q = 0.85$ (long dashed-short dashed line), and $q = 1/\sqrt{2}$ (dotted line). The standard $v_0 = 220$ km/s isothermal model (solid line) is shown for reference. See figure 10 and the text for more details.

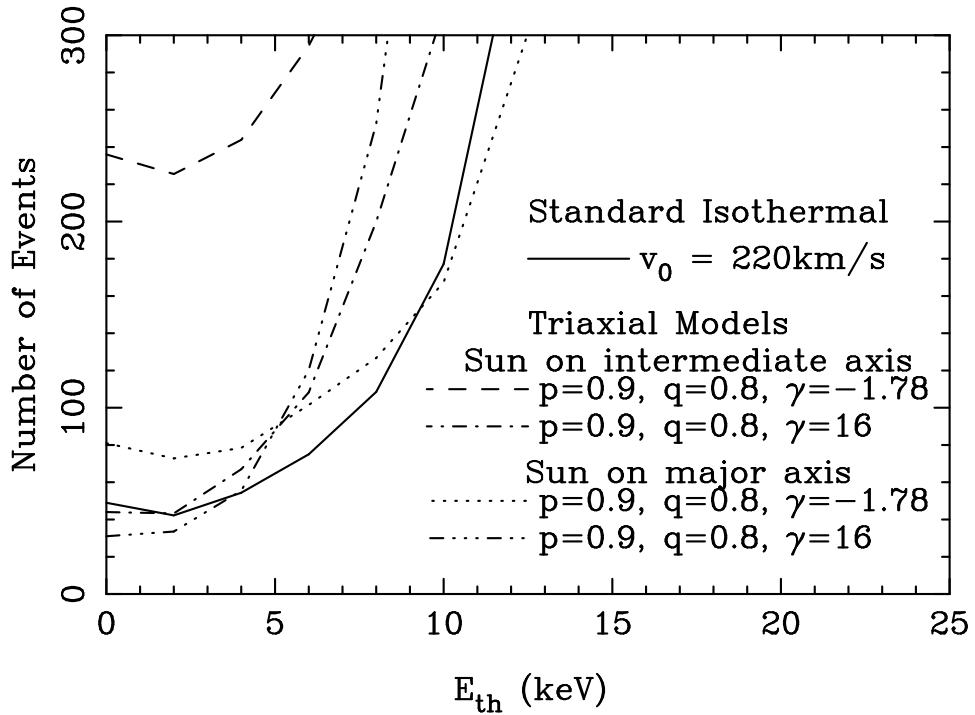


FIG. 16. The number of signal events required as a function of threshold energy to distinguish a triaxial distribution of WIMPs in the halo from a flat background using only the forward to backward ratio. Here we have considered a the Sun on the intermediate axis with $\gamma = -1.78$ (dashed line) and $\gamma = 16$ (long dashed-short dashed line) and the Sun on the major axis with $\gamma = -1.78$ (dotted line) and $\gamma = 16$ (dashed-dotted line). The standard $v_0 = 220$ km/s isothermal model (solid line) is shown for reference. See figure 11 and the text for a discussion.